www.czasopisma.pan.pl PAN www.journals.pan.pl
Opto-Electronics Review 25 (2017) 229–237

Contents lists available at ScienceDirect

Opto-Electronics Review

journal homepage: http://www.journals.elsevier.com/opto-electronics review

A new direction in design and manufacture of co-sensitized dye solar cells: Toward concurrent optimization of power conversion efficiency and durability

M. Hosseinnezhad [a,*], A. Shadman [b], M. Reza Saeb [c,*], Y. Mohammadi [d]

[a] Department of Organic Colorants, Institute for Color Science and Technology, P.O. Box 16656118481, Tehran, Iran
[b] Department of Industrial Engineering, Ferdowsi University of Mashhad, P.O. Box 91775-1111, Mashhad, Iran
[c] Department of Resin and Additive, Institute for Color Science and Technology, P.O. Box 16656118481, Tehran, Iran
[d] Petrochemical Research and Technology Company (NPC-rt), National Petrochemical Company (NPC), P.O. Box 14358-84711, Tehran, Iran

ARTICLE INFO

Article history:
Received 16 July 2016
Accepted 26 October 2016
Available online 23 July 2017

Keywords:
Dye-sensitized solar cell
Co-sensitization
Response surface methodology
Organic dye
Desirability function

ABSTRACT

A novel methodology was implemented in the present study to concurrently control power conversion efficiency (η) and durability (D) of co-sensitized dye solar cells. Applying response surface methodology (RSM) and Desirability Function (DF), the main influential assembling (dye volume ratio and anti-aggregation agent concentration) and operational (performance temperature) parameters were systematically changed to probe their main and interactive effects on the η and D responses. Individual optimization based on RSM elucidated that D can be solely controlled by changing the ratio of vat-based organic photosensitizers, whereas η takes both effects of dye volume ratio and anti-aggregation concentration into account. Among the studied factors, the performance temperature played the most vital role in η and D regulation. In particular, however, multi-objective optimization by DF explored the degree to which one should be careful about manipulation of assembling and operational parameters in the way maximization of performance of a co-sensitized dye solar cell.

1. Introduction

At the present time, the main concern of researchers is to find energy sources with minimum possible contamination toward the environment. Following the pioneering work by O'Regan and Gratzel in 1991 [1], exploration of dye-sensitized solar cells (DSSCs) as environmental-friendly devices capable of generating electron with receive photon from sun light, diverse publications were directed towards improvement of photovoltaic performance of DSSCs manipulating various operational and assembling parameters [2,3]. In general, dye monolayer chemicals were considered to play the role of a material parameter that could govern the performance of DSSCs [4]. In addition, the use of organic dye precursors brought the benefits of low cost and facile dye synthesis, meanwhile a fairly high power conversion efficiency (η) [5,6]. Most of all, it was attempted to synthesize engineering dyes with acceptable light harvesting ability [7], minimum possible aggregation potential [8,9], as well as very low charge recombination tendency [10]. With this aim in view, miscellaneous organic dyes were examined among which are thiophene, indoline, coumarine, and cyanine [11]. Vat based organic dyes are a new class of DSSC sensitizers exhibiting superior thermal, chemical and photochemical resistance [12]. Vat compounds are classified by colour index 10 as dyes and pigments. Indigo and thioindigo and their derivatives are important members of this class. The parent molecules, indigos, are extracted from natural plants, even though their derivatives are mostly prepared industrially. On the other hand, thioindigo does not exist in the nature and has been synthesized over the past century [11,12].

Despite acceptable intensity associated with the use of individual organic sensitizers, the narrow range of absorption of solar spectrum places some limits on their application [13]. This situation has been resolved by introduction of co-sensitization approach, through which η of solar cell has been enhanced significantly [14,15]. Chang et al. fabricated a co-sensitized solar cell (Co-DSSC) and achieved efficiency of 6.70 percent, which was well above values reported for individual DSSCs [16]. Kumara et al. proposed the idea of mixing dyes in a solution containing organic and natural photosensitizers, thereby improved efficiency of Co-DSSCs up to 1.13 percent [17]. Nonetheless, the spectrum range was not still

* Corresponding authors.
E-mail addresses: hosseinnezhad-mo@icrc.ac.ir (M. Hosseinnezhad), saeb-mr@icrc.ac.ir (M.R. Saeb).

http://dx.doi.org/10.1016/j.opelre.2017.06.003
1230-3402/

wide enough to warrant a high light harvesting ability responsible for elevating the efficiency. This inability was arisen from disuse of blue hue organic dye in the studied systems.

To the best of our knowledge, there is no report on lab- or industrial- scale production of vat based Co-DSSCs. The merit of vat based organic dyes lies in their low molecular weight, as well as the ability to yield blue hue guaranteeing a wide wavelength interval. Nonetheless, aggregation of vat dyes leading to banned or reduced electron transfer from the exited dye molecules to the photoelectrode should be taken into account when designing Co-DSSCs [18]. From this perspective, it seemed essential to utilize anti-aggregation agents in fabrication of DSSCs. The literature provides useful information on to what extent concentration of anti-aggregation agent governs the η of DSSCs [19]. Since DSSC devices work on the basis of one sun illumination, temperature plays a key role in solar cell performance [20].

Although the importance of η of DSSCs has been noticed by the researchers and engineers alike, a few reported on durability (D) of such devices, in spite of its vital importance from an application point of view. Takada et al. [21] and Lin et al. [22] noticed some points to improve D of DSSCs. Accordingly, it was found that utilization of carbon as working electrode or Pt as counter electrode improves the D of DSSCs. Nonetheless, available reports still lack a complete view on how D of DSSCs can be optimized by manipulating operational and assembling variables. An alternative method would be application of Co-DSSCs in which two vat-based organic dyes are mixed together and applied directly instead of sequentially. In a previous work we reported on enhancement of cell efficiency when using two dyes with respect to the case each dye was applied [23]. Nevertheless, the role of assembling and operating parameters has not been studied.

In the present work, we systematically changed volume ratio of dyes, performance temperature, and concentration of Cheno anti-aggregation agent to fabricate a series of Co-DSSCs to control η and D of Co-DSSCs using Response Surface Methodology (RSM) and Desirability Function (DF). Such combinatorial approach has been successfully applied by others for solving different multi-criteria optimization problems [24–26]. On the basis of RSM, volume ratio of vat-based organic dyes in a binary dye solution, concentration of anti-aggregation agent, and performance temperature were changed systematically, as explanatory variables, to enable concurrent control of η and D of Co-DSSCs. Of note, the idea of manufacturing Co-DSSCs with maximum attainable η and D has been disclosed here for the first time. Statistical analyses based on first-order, first-order with interaction, and second-order regression functions provided a detailed information about dependency of Co-DSSCs on performance temperature, which is the key finding of this work. Multi-objective optimization of the aforementioned targets by DF approach draws a new direction in identifying the individual and interactive effects of assembling and operational variables on η and D of Co-DSSCs.

2. Experimental design and statistical analyses

All ingredients used in synthesis and preparation of solar cells were analytical grades provided by Merck Co. and used as received. The two organic dyes, hereafter referred to as Dye 1 (indigo dye) and Dye 2 (thioindigo dye), innovatively synthesized and fully characterized in our previous papers were also used without further treatment [12,27]. These organic dyes were manufactured on the basis of indoxyl and thioindoxyl, respectively, through standard reactions and purified. Different mixtures of the assigned dyes were applied in production of Co-DSSCs.

To investigate the performance of manufactured Co-DSSCs, action spectra corresponding to each device were measured under monochromatic light with a constant photon number (5×10^{15} photon cm^{-2} s^{-1}). Photocurrent-photovoltage (J-V) characteristics of devices was measured under illumination with AM 1.5 simulated sun light (100 mW cm^{-2}) through a shading mast (5.0 mm × 4 mm) by using a Bunko-Keiki CEP-2000 system.

Table 1
Experimental range and coded levels of independent variables.

Variable	Symbols	Unit	Ranges and levels		
			−1	0	1
Volume of Dye1	A	(mL)	0	2.5	5
Performance-temperature	B	(°C)	10	30	50
Concentration of anti-aggregation agent	C	(mM)	0	10	20

In the light of previous studies, three explanatory variables including volume ratio of organic dyes (Dye 1/Dye 2), concentration of anti-aggregation agent, and performance-temperature were selected, as the most influential factors governing the η and D of DSSCs, and changed (Table 1). Since total volume of dye mixtures was unconditionally kept constant at 5 mL, we detected variations in η and D as a function of Dye 1 vol. Obviously, the volume of Dye 2 in the mixture can be simply calculated subtracting volume of Dye1 by total volume of 5 mL.

Application of RSM enabled systematic evaluation of the effects of chosen assembling and operational parameters, nominated as A, B, and C in Table 1, on the η and D of Co-DSSCs.

In general, first and second-order regression functions are suitable for analyzing the problem of interest, as follows [28]:

$$y = \beta_0 + \beta_1 x_1 + \beta_2 x_2 + \ldots\ldots\ldots \beta_k x_k + \varepsilon \quad (1)$$

$$y = \beta_0 + \sum_{j=1}^{k} \beta_j x_j + \sum_{j=1}^{k} \beta_{jj} x_j^2 + \sum \sum_{i<j=2}^{k} \beta_{ij} x_i x_j + \varepsilon. \quad (2)$$

In the above formulas, x and y are indicative of changing and response variables, respectively. Approximating functions take noises or errors in prediction of response variable into account in terms of ε in Eqs. (1) and (2). The coefficients β_1, β_2, …, and β_k in Eq. (1) take the main effects of changing variables on the selected response variable (in the current work η or D), while coefficients β_{jj} and β_{ij} in Eq. (2) are known as curvature and interaction terms reflecting the interactive effects between changing variables, respectively. When one has aimed at investigating the interaction between changing variables, quadratic interpolation function could provide more information about actual effects of parameters [29–32].

According to variation levels proposed by RSM, fifteen solar cells were manufactured and their η and D were measured and tabulated. Based on three-factor Box-Behnken Design (BBD), fifteen experiments were designed as represented in Table 2. Design Expert software package version 7 was used for design analysis and optimization.

In case of RSM, three types of regression functions were applied to experimental data: (*i*) linear model; (*ii*) linear model with interactions; and (*iii*) quadratic model. The coefficient of determination (R-squared or R^2) and adjusted R^2 (Adjusted-R^2) were compared in each case to indicate which model brings more precision among all studied models. In addition, depending on the selected response, the reduced form of the regression function was considered through which a better fit was obtained. Accordingly, we realized which factors, independently or simultaneously affect the η and D target variables.

The set of optimal solutions was obtained, in the second step of optimization, with the aid of multi-criteria optimization by DF

Table 2
Different experiments proposed by the RSM to be performed.

Experimental runs	A	B	C	η (%)	D (h)
1	5	30	20	2.72	1700
2	2.5	30	10	6.58	1100
3	5	50	10	3.65	1600
4	2.5	50	0	5.32	800
5	2.5	10	20	5.74	1200
6	5	30	0	3.45	1800
7	2.5	50	20	4.59	600
8	0	30	20	4.97	700
9	2.5	30	10	6.58	1000
10	0	50	10	5.99	600
11	0	10	10	7.19	800
12	5	10	10	4.91	1900
13	2.5	10	0	6.68	1300
14	0	30	0	5.81	800
15	2.5	30	10	6.59	1100

approach on quadratic mathematical models obtained by RSM [24]. Derringer and Suich proposed three types of individual desirability functions, namely Nominal-The-Best (NTB), Larger-The-Best (LTB), and Smaller-The-Best (STB) [33]. The dimensionless desirability value d is defined as the transformed value of the measured properties of each predicted response y. In case of LTB, the desirability is defined as follows:

$$d = \left|\frac{y-L}{U-L}\right|^{\alpha},\ L \le y \le U,\ \text{with } d = 0 \text{ for } y < L \text{ and}$$
$$d = 1 \text{ for } y > U\ . \tag{3}$$

Likewise, in case of STB the desirability is defined as:

$$d = \left|\frac{y-U}{L-U}\right|^{\alpha},\ L \le y \le U,\ \text{with } d = 0 \text{ for } y > U \text{ and}$$
$$d = 1 \text{ for } y > L\ . \tag{4}$$

In the above relations, α is a user-specified parameter that takes a non-zero value, while L and U are specified depending on the mathematical model obtained through RSM. To perform multi-objective optimization, a single criterion is created aggregating the individual desirability functions (d_i) into a weighted geometric mean composite desirability function (CD) [34]:

$$CD = \left((d_1)^{w_1}(d_2)^{w_2}\ldots\left(d_p\right)^{w_p}\right)^{\frac{1}{\sum w_i}} \tag{5}$$

where w_i quantities reflect the priorities in the importance of d_i functions. The objective in multi-objective optimization is to maximize the CD ($CD = 1$) corresponding to the case when all responses are on-target ($d_i = 1$). On the other hand, CD takes value of zero when at least one response is outside of the specification limits ($d_i = 0$, for any i). For intermediate cases, the CD takes a value less than or equal to the lowest value of d_i. Thus, the CD ranges between 0 and 1, respectively suggesting unacceptable and exactly target values. Depending on the goodness of balance between d_i quantities, an increase in value of CD is expected [35].

3. Results and discussion

First, photovoltaic properties of each device are measured and compared to find through a crude approximation the association between co-sensitization behavior and performance of co-DSSCs. All devices are investigated under the standard global AM 1.5 solar condition [36]. The DSSCs with co-sensitization of Dye1/Dye2 revealed, at best, power conversion efficiency of ca. 6.17% at Dye1/Dye2 vol ratio of 2/3. The corresponding value for co-DSSCs in the presence of anti-aggregation agent has increased to 6.82%. The effect of temperature on DSSCs performance has also been viewed. Of note, characterization of DSSCs is performed at ambient temperature (25 °C), while the temperature in practical applications is above this value. To assess this, higher temperatures were applied in construction, where photovoltaic properties decreased with increase of the temperature.

To find the criterion under which η and D both take the maximum possible quantities, it is essential to optimize each response individually. As described in the previous sections, the use of a mixture of dyes itself brings the benefit of broadening the light absorption interval [37,38]. The most critical question to be answered is whether or not a set of optimized assembling and operational parameters maximizing one target would unconditionally maximize the other target. In the following, we describe in details the procedure of finding the best interpolating function describing the behaviour of η and D over the experimental range of explanatory variables A, B, and C defined in Table 1. On the basis of analysis of variance (ANOVA), the reliability of the proposed mathematical model by RSM will be determined and, if necessary, the reduced models with higher degree of reliability will be suggested in each case. The order of significance of the changing variables, individually or interactively, as well as bivariate contour plots are provided for better understanding of sensitivity of each response variable to the cell performance parameters. Taking into consideration the mathematical models obtained through RSM, the multi-criteria optimization by DF approach will specify to what extent combination of RSM and DF helps for manufacturing high-performance Co-DSSCs.

3.1. Individual optimization of targets by RSM

Typically, the analysis of RSM has three steps: (*i*) finding a response function, (*ii*) interpreting the obtained model; and (*iii*) identifying the optimum criteria. We applied different models to the experimental data to find the best interpolating function among possible cases when using BBD methodology [29,30]. Interpretations were based on the reduced model obtained through statistical interpretation of the results.

3.1.1. Analysis of η

Application of Design Expert software indicated that the quadratic model provides the best regression function among examined patterns as realized from sequential sum of squares and lack of fit tests. Table 3 shows the ANOVA for the reduced quadratic model obtained for η, in which the p-value of the model is very meaningful (< 0.0001). In this table, all predictors are meaningful and the p-value of the lack of fit test (0.0518) replies on the adequacy of model. The R-squared value of 0.9999 demonstrates that 99.99 percent of variability of the gathered data can be expressed by the linear model, which is acceptable.

The reduced quadratic model applied to the real experimental data is given in Eq. (6). The main, interaction, contour and response surface plots were inspired from the obtained model and employed to further investigate η response.

$$\begin{aligned}\eta = {} & 7.05563 + 0.52483 \times Dye1 + 0.16871 \\ & \times C - 0.048438 \times T + 0.0011 \times Dye1 \times C \\ & + 0.000262 \times T \times C - 0.19947 \times Dye1^2 - 0.010992 \\ & \times C^2 + 0.0002458 \times T^2\end{aligned} \tag{6}$$

It can be realized from Eq. (6) that the chosen manufacturing parameters are distinctly and interactively contributed to the variability η, for both curvature and interaction terms are appeared in the quadratic model. Therefore, power conversion efficiency is highly sensitive to the chosen manufacturing parameters. In such situation, the coin of η optimization has a promising head on one side and a critical tail on the other. The involvement of almost

Table 3
ANOVA table assigned to quadratic model relating to η response.

Source	Sum of Squares	df	Mean Square	F Value	p-value Prob > F	
Model	24.80	8	3.10	7319.22	<0.0001	significant
A-Dye1/Dye2	10.65	1	10.65	25138.89	<0.0001	–
B-T	3.09	1	3.09	7288.79	<0.0001	–
C–C	1.31	1	1.31	3097.65	<0.0001	–
AC	3.025E-003	1	3.025E-003	7.14	0.0369	–
BC	0.011	1	0.011	26.03	0.0022	–
A^2	5.74	1	5.74	13546.63	<0.0001	–
B^2	0.036	1	0.036	84.28	<0.0001	–
C^2	4.46	1	4.46	10530.71	<0.0001	–
Residual	2.542E-003	6	4.236E-004	–	–	–
Lack of Fit	2.475E-003	4	6.187E-004	18.56	0.0518	not significant
Pure Error	6.667E-005	2	3.333E-005	–	–	–
Cor Total	24.81	14	–	–	–	–
Std. Dev.	0.021	–	R-Squared	0.9999	–	–
Mean	5.38	–	Adj R-Squared	0.9998	–	–
C.V.%	0.38	–	Pred R-Squared	0.9989	–	–
PRESS	0.027	–	Adeq Precision	282.4980	–	–

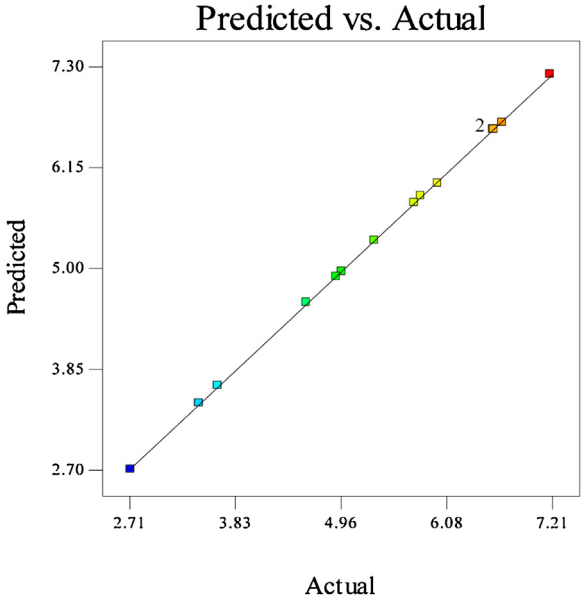

Fig. 1. Predicted values of η vs. actual values based on Eq. (6).

all possible terms in Eq. (6) provides a wider range of freedom in working with manufacturing variables, meanwhile a stronger dependency of η on very small changes in them. The predictability of the reduced model toward η is featured in Fig. 1. It is apparent that Eq. (6) can exactly predict the behaviour of η over experimental range considered in the current work for manufacturing variables.

Fig. 2a illustrates bivariate plots of η as a function of anti-aggregation agent concentration and dye volume ratio at different manufacturing temperatures. The main finding is that the studied manufacturing parameters have a substantial impact on the η of solar cells. The significant colour change observed for plots provided at different temperatures is a signature of dependency of η on characterization temperature. In other words, increase of manufacturing temperature adversely affects the η, which is featured in disappearance of reddish regions. It is also apparent from plots in Fig. 2a that obtaining high values of η could be associated with low or intermediate values for anti-aggregation agent concentration and dye volume ratio.

According to Arrhenius law, the diffusion coefficient of electron to nanostructured substrate increases exponentially with temperature and, through which, a rise in short circuit current (J_{SC}) would be expected [19]. On the other hand, according to the Metal Ligand Charge Transfer (MLCT) effect [20], increase of temperature could reduce the charge recombination at dye-photoelectrode interface, thereby provides a higher V_{OC} value. There is sufficient evidence that a strong recombination governs the performance of DSSCs by lowering the J_{SC} [12]. In addition, the η of DSSCs resembles more and less the J_{SC} behaviour. As a result, as in Fig. 2a, the η of DSSCs declines upon increase of temperature. It is believed that the results of this study visualize in an appropriate way this fact. Overall, statistical evaluations revealed that for maximizing the value of η in the studied range of variables, manufacturing parameters have to be adjusted as: T = 10, Dye1/Dye2 = 1.34/3.66 and $C = 7.86 \times 10^{-3}$.

3.1.2. Analysis of D

Experimental data summarized in Table 2 suggest that η and D values of DSSCs devices are almost moved in an adverse direction. This is mostly reported for solar cells, and places some serious limitations on the use of these devices. It can be realized from the statistical criteria in Table 4 that a reduced quadratic model, containing less terms compared to Eq. (6), satisfactorily describes variation behaviour of D response over the experimental test bounds. Table 4 shows that the linear effects of all factors and the quadratic effect of Dye1/Dye2 are meaningful. Noticeably, however, A, B, and C explanatory variables have shown no interactive effects on D target. This indicates that manufacturing parameters have somewhat different effect on the studied responses. The reduced approximating function predicting D variation with individual and quadratic coefficients is given through Eq. (7):

$$D = 1087.5 + 26.42758 \times Dye1 - 6.2500 \times C - 10.0000 \times T + 35.71429 \times Dye1^2 \quad (7)$$

The goodness of the obtained quadratic model in predicting response D is illustrated through Fig. 3. A first glimpse at the plot confirms that at lower values of D, which is roughly the case where η takes the highest possible quantities, the model suffers from insufficient precision.

Contour plots of D response are provided in Fig. 2b. It is obvious that the behaviour of D response over the studied range of variables is different in comparison with the η with circular contours. This indicates that D criterion has not been influenced by the anti-aggregation agent concentration. Even at a low temperature of 10 °C, the red zone is situated on the top of the plot, where a mixture mostly contained of Dye1, irrespective of anti-aggregation agent content, gives the opportunity for maximizing D response. Thus, it can be concluded that Dye1 and Dye2 are responsible for maximizing the D and η of DSSCs, respectively. This can be simply

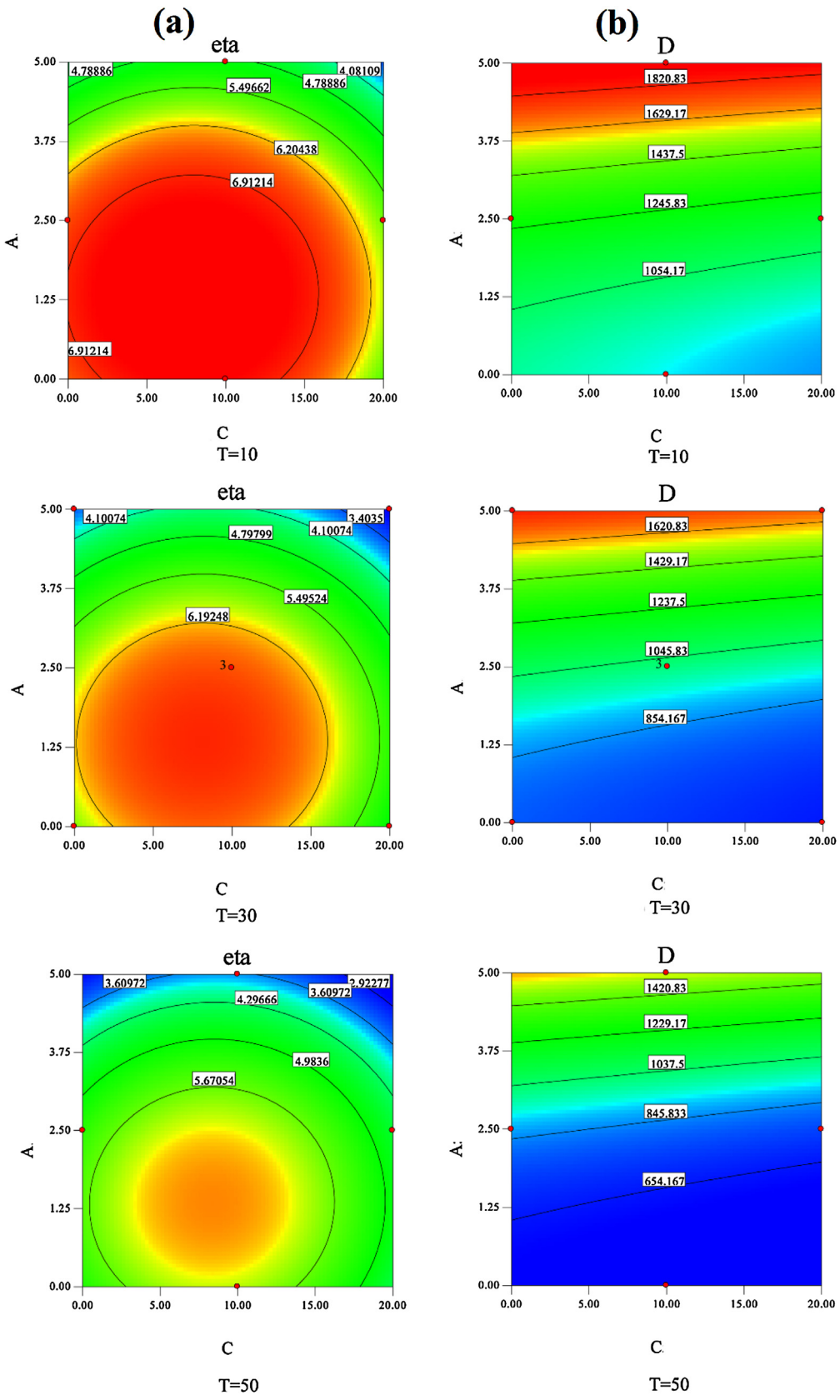

Fig. 2. Contour plots of η {(a) series plots on the left side} and D {(b) series blots on the right side} in terms of ante-aggregation agent concentration and dye volume ratio at different manufacturing temperature levels.

Table 4
ANOVA table assigned to the reduced quadratic model relating to D response.

Source	Sum of Squares	df	Mean Square	F Value	p-value Prob > F	
Model	2.639E+006	4	6.596E+005	88.16	<0.0001	significant
A-Dye1	2.101E+006	1	2.101E+006	280.84	<0.0001	
B-T	3.200E+005	1	3.200E+005	42.77	<0.0001	
C-C	31250.00	1	31250.00	4.18	0.0682	
A^2	1.860E+005	1	1.860E+005	24.86	0.0005	
Residual	74821.43	10	7482.14	–	–	
Lack of Fit	68154.76	8	8519.35	2.56	0.3115	not significant
Pure Error	6666.67	2	3333.33	–	–	
Cor Total	2.713E+006	14	–	–	–	
Std. Dev.	86.50	–	R-Squared	0.9724	–	
Mean	1133.33	–	Adj R-Squared	0.9614	–	
C.V.%	7.63	–	Pred R-Squared	0.9342	–	
PRESS	1.785E+005	–	Adeq Precision	28.5340	–	

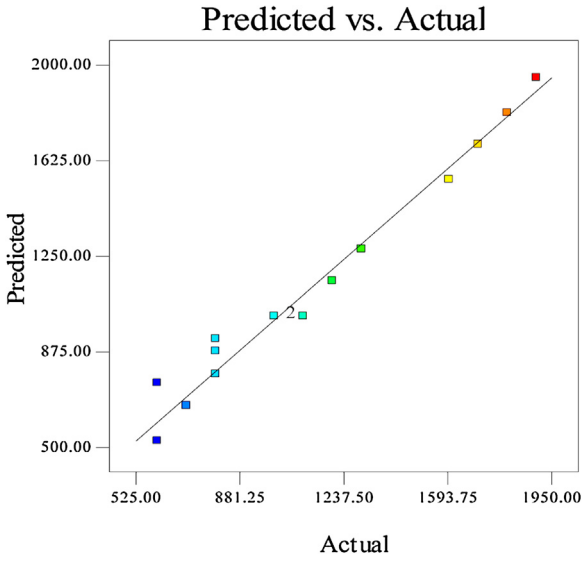

Fig. 3. Predicted values of D vs. actual values based on Eq. (7).

accepted comparing the D and η values of solar cells manufactured based on experimental runs 11 and 12 in Table 2. In a similar fashion, comparison between D and η values of experiments 5 and 13 in the assigned table suggests that anti-aggregation agent has a negligible effect on the performance of Co-DSSCs.

For the sake of further explanation, it should be noticed that D depends not only on the chemical stability of organic dyes, but also on how tightly they are anchored covalently to the nanostructured substrate [20]. In general, vat based dyes are known because of their excellent thermal, chemical and photochemical stability, which is expected to strengthen the D of solar cells. Nonetheless, factors affecting D and η are almost acting in different directions. Typically, the stability of indigo dyes (here Dye1) is higher than of thioindigo dyes (here Dye2) [21]. As a result, it is expected to yield larger D values when the mixture is mostly containing Dye1, which is in full agreement with our observations.

3.2. Multi-criteria optimization of targets by DF

The results presented and discussed in the previous section demonstrated that factors affecting D and η somehow act in different directions so as to make difficult multi-objective optimization of cell performance. Application of DF technique reflects to what extent a given problem allows for such optimization. Accordingly, η and D are changed to d_1 and d_2 desirabilities to be correlated with the *CD* defined as:

$$CD = (d_1.d_2)^{\frac{1}{2}} \tag{8}$$

The desirability is then interrelated to the nature of the problem. Since the η took values in the range 2.72–7.62, this interval should principally have the target desirability. The maximum desirability was set to take a value greater than 7.62, hence, d_1 can be defined as:

$$d_1 = \begin{cases} 0 & ; y_1 < 2.72 \\ \dfrac{y_1 - 2.72}{4.47} & ; 2.72 \le y_1 \le 7.19 \\ 1 & ; y_1 > 7.19 \end{cases} \tag{9}$$

For the second response variable, since the D has taken values in the range 600–1900, this interval has the target desirability. The maximum desirability was allowed for taking valuea greater than 1900, hence, d_2 can be defined as:

$$d_2 = \begin{cases} 0 & ; y_2 < 600 \\ \dfrac{y_2 - 600}{1300} & ; 600 \le y_2 \le 1900 \\ 1 & ; y_2 > 1900 \end{cases} \tag{10}$$

In this regard, the quantities of changing variables are manipulated to meet the highest *CD* value, as far as possible close to unity. This has been carried out by Design Expert software. A number of the best solutions among the ones proposed by the software are listed in Table 5.

As can be seen, the results are sorted in accord with desirability, however, they are closely suggesting a unique solution, that is η = 6.2% and D = 1620 h, which are achieved at Dye1/Dye2 = 4/1, T = 10 °C, and C = 7 mM. Particularly interesting are the levels suggested for explanatory variables through multi-criteria optimization by DF approach, which are completely different with those proposed by RSM based on individual optimization of each response. In other words, in contrast to single-objective problems, a mixture of Dye1 and Dye2 is needed for taking full advantages of η and D targets. From this perspective, development of Co-DSSCs devices would be reasonable, while individual optimization technique still suggests application of single DSSCs. The overlay plots obtained for cases with different manufacturing temperature, i.e. levels of 10, 30 and 50 °C, shed more light on the reasonability of using Co-DSSC devices (Fig. 4). Overlay plots are contour plots at which the yellowed region signifies the place where both responses take the desired values. Fig. 4 indicates that η and D could not be concurrently controlled at the predetermined levels if temperature was 30 or 50 °C. On the other hand, at T = 10 °C the plot has a yellow zone at which η and D values are simultaneously maximized.

Table 5
Desirability functions corresponding to the best cases of design with both responses being optimized.

Solution No.	Dye1/Dye2 vol ratio(−)	T (°C)	C (mM)	η (%)	D (h)	Desirability	
1	4.00/1.00	10.00	7.02	6. 19,650	1620.53	0.715	Selected
2	3.97/1.03	10.00	6.83	6. 22,624	1611.65	0.715	
3	3.94/1.06	10.00	6.94	6. 25,493	1603.26	0.715	
4	3.94/1.06	10.00	7.20	6. 26,036	1601.59	0.715	
5	3.93/1.07	10.00	7.11	6. 26,798	1599.41	0.715	
6	4.06/0.94	10.00	7.41	6. 13,710	1637.40	0.715	

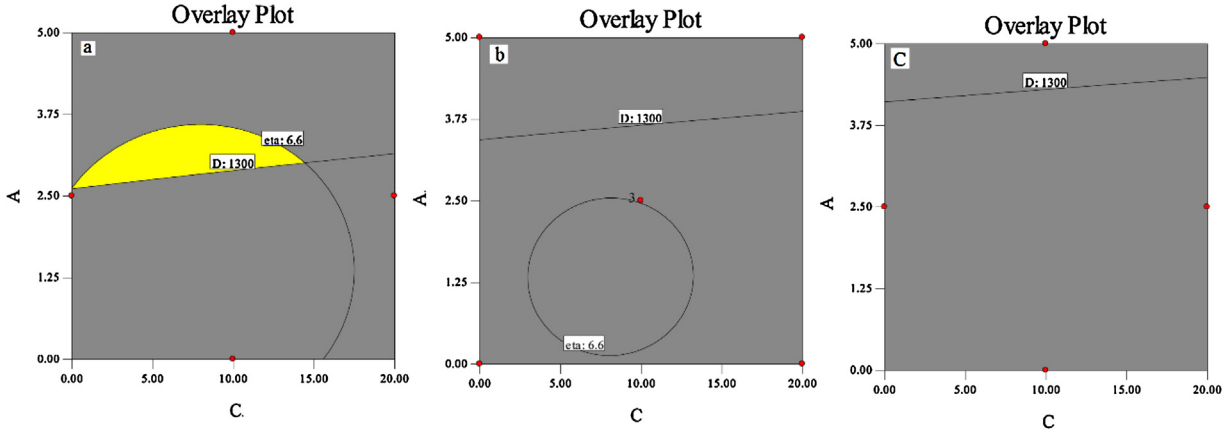

Fig. 4. Overlaid plots illustrating the optimized regions yielded at constant T levels of 10 (a), 30 (b), and 50 °C (c) to maintain the η and D in the range of 6.6–7.7 and 1300–1900, respectively.

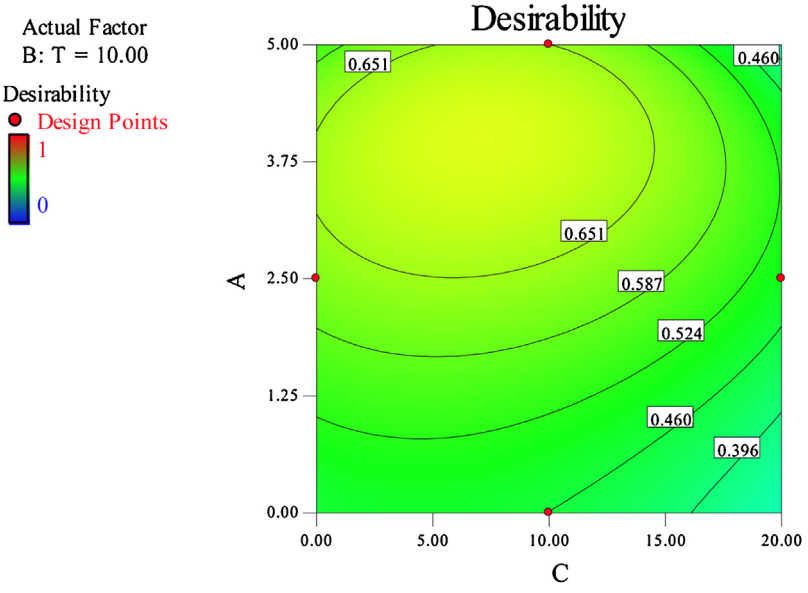

Fig. 5. Contour plots of desirability corresponding to simultaneous optimization of η and D.

Noticeably, a 2.5/2.5 mixture of dyes allows for such multi-criteria optimization, which is in vivid opposition to the equivalent plot in Fig. 2b.

From the perspective drawn in this work some new windows are opened to be taken when concurrent control of η and D is the goal. Contour plots corresponding to the different desirabilities when optimizing both targets are drawn in Fig. 5.

In agreement with the results in Table 5, the potential of system to yield desirability of unity is undeniably limited. Despite this, hybridization of RSM and DF methodologies visualized the capability of polynomial-based approximating functions in tracking and optimizing both η and D targets.

Overall, the usefulness of the applied technique to optimize both η and D targets has been visualized in Fig. 6. The sketch shows that by lowering the manufacture temperature the likelihood of simultaneous control of η and D rises. The illustration shows that for Co-DSSCs having dye ratio of 2.5/2.5, the possibility of concurrently keeping η and D well above a satisfactory level rises at low manufacture temperatures. Noticeably, manipulation of manufacturing temperature has a negligible effect on the V_{OC}, while significantly determines the J_{SC} value. Since the latter criterion is directly in relationship with the η of Co-DSSCs, fine-tuning of η can be somehow solely achieved by lowering the manufacturing temperature. The interesting point, however, would be the possibility of man-

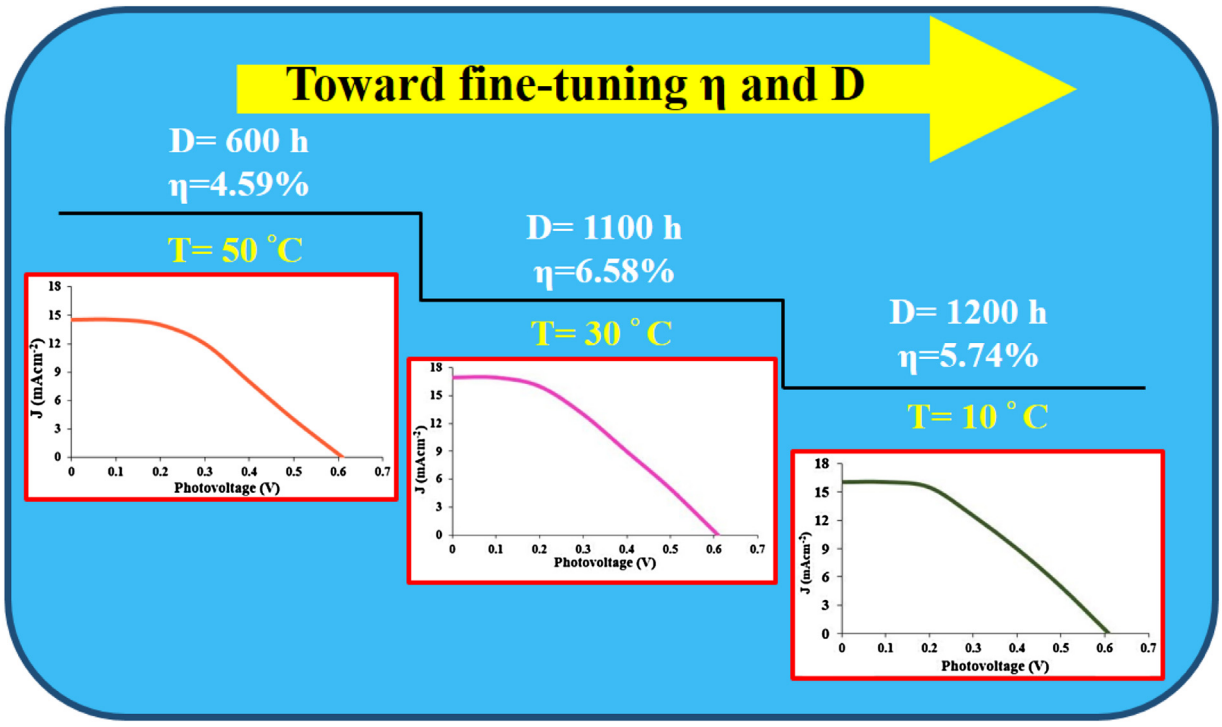

Fig. 6. Illustrative visualization of the temperature effect on the performance Co-DSSCs with 2.5/2.5 Dye1/Dye2 vol ratio.

ufacturing co-DSSCs, instead of DSSCs having only one vat based dye, in which the other operational property, that is D, takes values well above those conventionally observed for DSSCs. Thus, it makes evident that the use of Co-DSSCs devices with two dyes, each responsible for obtaining the desired η or D, is reasonable, if one can appropriately tune the level of assembling and operational parameters to hit both predetermined values η or D targets.

4. Conclusions

A combination of RSM and DF approaches was employed to control concurrently η and D of co-dye-sensitized solar cells (Co-DSSCs). Application of indigo and thioindigo vat dyes, respectively coded as Dye1 and Dye2, enabled co-sensitization of the photoanode of DSSCs. The RSM was used to design an experimental plane, where volume ratio of organic dyes, anti-aggregation agent content and temperature were changing variables, while η and D of Co-DSSCs were response variables. Typical R-squared values very close to unity, assigned to the reduced second-order models obtained for η and D, reflected the capability of RSM in capturing the variation in η or D. The impact of manufacturing temperature on the η and D of co-DSSCs has been visualized, so as to a mixture mainly composed of Dye2 and Dye1 was responsible for achieving the maximal values for η or D, respectively. With the help of overlaid plots yielded from multi-objective optimization of η and D, however, it was realized that a mixture of Dye1 and Dye2 is needed to enhance both η and D at manufacturing temperature of 10 °C. The use of DF enabled simultaneous enlargement of η and D to a reasonable degree, which has not been reported yet before.

References

[1] B. O'Regan, M. Gratzel, A low cost, high-efficiency solar cell based on dye-sensitized colloidal TiO_2 films, Nature 353 (1991) 737–740.
[2] N. Asim, K. Sopian, S. Ahmadi, K. Saeedfar, M.A. Alghoul, O. Saadatian, S.H. Zaidi, A review on the role of materials science in solar cells, Renew. Sustain. Energy Rev. 16 (2012) 5834–5847.
[3] M. Gratzel, Dye-sensitized solar cells, J. Photochem. Photobiol. C: Photochem. Rev. 4 (2003) 145–153.
[4] X. Wang, Z.M. Wang, High Efficiency Solar Cells: Physics, Materials and Devices, Springer, Switzerland, 2014.
[5] J. Gong, J. Liang, K. Sumathy, Review on dye-sensitized solar cells (DSSCs): fundamental concepts and novel materials, Renew. Sustain. Energy Rev. 16 (2012) 5848–5860.
[6] G.J. Conibeer, A. Willoughby, Solar Cell Materials Developing Technology, John Wiley & Sons, United Kingdom, 2014.
[7] G.D. Sharma, P.A. Angaridis, S. Pipou, G.E. Zervaki, V. Nikolaou, R. Misra, A.G. Coutsolelos, Efficient co-sensitization of dye-sensitized solar cells by novel porphyrin/triazine dye and tertiary aryl-amine organic dye, Org. Electron. 25 (2015) 295–307.
[8] M. Hosseinnezhad, S. Moradian, K. Gharanjig, Investigation of effect of anti-aggregation agent on the performance of nanostructure dye-sensitized solar cells, Opto-Electron. Rev. 23 (2015) 126–130.
[9] A.R.K. Selvaraj, S. Hayase, Molecular dynamics simulations on the aggregation behavior of indole type organic dye molecules in dye-sensitized solar cells, J. Mol. Model. 18 (2012) 2099–2104.
[10] T. Daeneke, A.J. Mozer, T. Kwon, N.W. Duffy, A.B. Holmes, U. Bach, L. Spiccia, Dye regeneration and charge recombination in dye-sensitized solar cells with ferrocene derivatives as redox mediators, Energy Environ. Sci. 5 (2012) 7090–7099.
[11] M. Mishra, M.K.R. Fischer, P. Bauerle, Metal free organic dyes for dye-sensitized solar cells: from structure: property relationships to design rules, Angew. Chem. Int. Ed. 48 (2009) 2474–2499.
[12] M. Hosseinnezhad, S. Moradian, K. Gharanjig, Novel organic dyes based on thioindigo for dye-sensitized solar cells, Dyes Pigm. 123 (2015) 147–153.
[13] J. Yum, E. Baranoff, S. Wenger, M.K. Nazeeruddin, M. Gratzel, Panchromatic engineering for dye-sensitized solar cells, Energy Environ. Sci. 4 (2011) 842–857.
[14] Q. Shen, Y. Ogomi, B. Park, T. Inoue, S.S. Pandey, A. Miyamoto, S. Fujita, K. Katayama, T. Toyod, S. Hayase, Multiple electron injection dynamics in linearly-linked two dye co-sensitized nanocrystalline metal oxide electrodes for dye-sensitized solar cells, Phys. Chem. Chem. Phys. 14 (2012) 4605–4613.
[15] A. Baheti, P. Singh, C. Lee, K.R.J. Thomas, K. Ho, 2,7-Diaminofluorene-based organic dyes for dye-sensitized solar cells: effect of auxiliary donor on optical and electrochemical properties, J. Org. Chem. 76 (2011) 4910–4920.
[16] J. Chang, C.P. Lee, D. Kumar, P.W. Chen, L.Y. Lin, K.R.J. Thomas, K.C. Ho, Co-sensitized solar cells using unsymmetrical squarain dyes and novel pyrenoimidazole-based dye, J. Power Sources 240 (2013) 779–785.
[17] N.T.R.N. Kumara, P. Ekanayake, A. Lim, L.Y.C. Llew, M. Iskandar, L.C. Ming, G.K.R. Senadeera, Layered co-sensitization for enhancement of conversion efficiency of natural dye sensitized solar cells, J. Alloys Compd. 581 (2013) 186–191.
[18] E.M. Barea, J. Bisquert, Properties of chromophores determining recombination at the TiO_2-dye-electrolyte interface, Langmuir 29 (2013) 877–878.

[19] M. Hosseinnezhad, K. Gharanjig, S. Moradian, Effect of anti-aggregation agent on photovoltaic performance of indoline sensitized solar cells, Mater. Technol. 30 (2015) 189–192.
[20] M. Berginc, U. Opara Krasovec, M. Hocevar, M. Topic, Performance of dye-sensitized solar cells based on ionic liquids: effect of temperature and iodine concentration, Thin Solid Films 516 (2008) 7155–7159.
[21] H. Takada, Y. Obana, R. Sasaki, M. Kuribayashi, M. Kanno, C. Zhu, T. Bessho, Y. Takagi, K. Hinokuma, K. Noda, Improved durability of dye-sensitized solar cells with H_2-reduced carbon counter electrode, J. Power Source 274 (2015) 1276–1282.
[22] L. Lin, C. Lee, R. Vittal, K. Ho, Improving the durability of dye-sensitized solar cells through back illumination, J. Power Source 196 (2011) 1671–1676.
[23] M. Hosseinnezhad, Improvement performance of dye sensitised solar cells from co-sensitisation of TiO_2 electrode with organic dyes based on indigo and thioindigo, Mater. Technol. 31 (2016) 348–351.
[24] J. Li, C. Ma, Y. Li, W. Zhou, P. Xu, Medium optimization by combination of response surface methodology and desirability function: an application in glutamine production, Appl. Microbiol. Biotechnol. 74 (2007) 563–571.
[25] E. Roszet, V. Wascotte, N. Lecouturier, V. Preat, W. Dewe, B. Boulanger, Ph. Hubert, Improvement of the decision efficiency of the accuracy profile by means of a desirability function for analytical methods validation: application to a diacetyl-monoxime colorimetric assay used for the determination of urea in transdermal iontophoretic extracts, Anal. Chim. Acta 591 (2007) 239–247.
[26] M. Mourabet, A. El Rhilassi, H. El Boujaady, M. Bennani-Ziatni, R. El Hamri, A. Taitai, Removal of fluoride from aqueous solution by adsorption on Apatitic tricalcium phosphate using Box-Behnken design and desirability function, Appl. Surf. Sci. 258 (2012) 4402–4410.
[27] M. Hosseinnezhad, S. Moradian, K. Gharanjig, Synthesis and characterization of two new organic dyes for dye-sensitized solar cells, Synth. Commun. 44 (2014) 779–787.
[28] D.C. Montgomery, Design and Analysis of Experiments, 6th ed., Wiley, New York, 2005.
[29] M.R. Saeb, M. Moghri, H.A. Khonakdar, U. Wagenknecht, G. Heinrich, Fusion level optimization of rigid PVC nanocompounds by using response surface methodology, J. Vinyl Addit. Technol. 19 (2013) 168–176.
[30] M. Moghri, M. Khakpour, M. Akbarian, M.R. Saeb, Employing response surface approach for optimization of fusion characteristics in rigid foam PVC/clay nanocomposites, J. Vinyl Addit. Technol. 21 (2015) 51–59.
[31] A.S. Pakdel, M.R. Behbahani, M.R. Saeb, H.A. Khonakdar, H. Abedini, M. Moghri, Evolution of vinyl chloride conversion below critical micelle concentration: a response surface analysis, J. Vinyl Addit. Technol. 21 (2015) 157–165.
[32] M. Ataeefard, M.R. Saeb, A multiple process optimization strategy for manufacturing environmentally friendly printing toners, J. Clean. Prod. 108 (2015) 121–130.
[33] N.R. Costa, J. Lourenco, Z.L. Pereira, Desirability function approach: a review and performance valuation in adverse conditions, Chemom. Intell. Lab. 107 (2011) 234–244.
[34] C. Cojocaru, M. Khayet, G. Zakrzewska-Trznadel, A. Jaworska, Modelling and multi-response optimization of pervaporation of organic aqueous solutions using desirability function approach, J. Hazard. Mater. 167 (2009) 52–63.
[35] K. Elsayed, C. Lacor, CFD modelling and multi-objective optimization of cyclone geometry using desirability function, artificial neural networks and genetic algorithms, Appl. Math. Model. 37 (2013) 5680–5704.
[36] M. Hosseinnezhad, S. Moradian, K. Gharanjig, Acid azo dyes for efficient molecular photovoltaic study of dye-sensitized solar cells performance, Prog. Color Colorants Coat. 9 (2016) 61–70.
[37] C. Lan, H. Wu, T. Pan, C. Chang, W. Chao, C. Chen, C. Wang, C. Lin, E. Diau, Enhanced photovoltaic performance with co-sensitization of porphyrin and an organic dye in dye-sensitized solar cells, Energy Environ. Sci. 5 (2012) 6460–6464.
[38] S.M. Shinda, D.C. Montgomery, B. Jones, Projection of no-confounding designs for six, seven and eight factors in 16 runs, Int. J. Exp. Des. Proc. Optim. 4 (2014) 1–26.